Transient and steady-state solutions of 2D viscoelastic nonisothermal simulation model of film casting process via finite element method

Dong Myeong Shin

Department of Chemical and Biological Engineering, Applied Rheology Center, Korea University, Seoul 136-713, Korea

Joo Sung Lee

Department of Chemical Engineering, University of California at Berkeley, Berkeley, California 94720

Ju Min Kim

Department of Chemical Engineering Massachusetts Institute of Technology, Cambridge, Massachusetts

Hyun Wook Jung and Jae Chun Hyun[a)]

Department of Chemical and Biological Engineering, Applied Rheology Center, Korea University, Seoul 136-713, Korea

(Received 31 July 2006; final revision received 18 January 2007)

Synopsis

The various aspects of the nonlinear dynamics and stability of nonisothermal film casting process have been investigated solving a two-dimensional (2D) viscoelastic simulation model equipped with the Phan-Thien-Tanner (PTT) constitutive equation by employing a finite element method. This study represents an extension of the earlier report [Kim, Lee, Shin, Jung, and Hyun, J. Non-Newtonian Fluid Mech. **132**, 53–60 (2005)] in that two important points are additionally addressed here on the subject: the nonisothermal nature of the film casting, and the differentiation of extension-thickening (strain hardening) and extension-thinning (strain softening) fluids in their different behavior in the film casting process. The PTT model, known for its robustness in portraying dynamics in the extensional deformation processes which include the film casting of this study along with film blowing and fiber spinning as well, renders the transient and steady state solutions of the dynamics in the 2D, viscoelastic, nonisothermal, film casting capable of explaining the effects of various process and material parameters of the system on the film dynamics of the process. Especially, the different behavior displayed by two polymer groups, i.e., the extension-thickening low density polyethylene (LDPE) type and the extension-thinning high density polyethylene (HDPE) type, in the film casting can be readily explained by the PTT equation-

[a)]Author to whom correspondence should be addressed; electronic mail: jchyun@grtrkr.korea.ac.kr

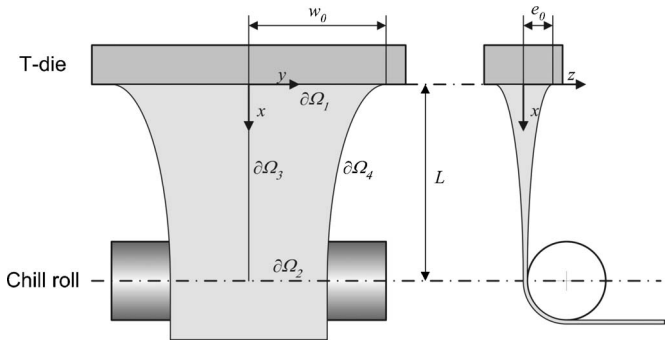

FIG. 1. Schematic geometry and boundaries of the process.

included simulation model. The three nonlinear phenomena commonly observed in film casting, i.e., draw resonance oscillation, edge bead, and neck-in, have been successfully delineated in this study using the simulation and experimental results.
[DOI: 10.1122/1.2714781]

I. INTRODUCTION

The film casting process is an industrially important polymer processing operation producing films, through continuously extruding a molten, thin polymer sheet from a slit die, stretching it along the machine direction and then cooling it on a chill roll (take-up device), as shown in Fig. 1. Enhancing the process productivity and the product film uniformity in this film casting always entails a thorough understanding of the dynamics and stability of the system because, as in any other industrial production processes, various kinds of disturbances inevitably affect the process stability and give rise to several defects of produced films through draw resonance instability, neck-in of the film width and edge bead on the film product. The draw resonance is a Hopf bifurcation instability manifesting itself as the periodic oscillation of the state variables like film thickness and width as the film draw ratio between the die exit and the chill roll exceeds certain critical values. This instability phenomenon occurring in other extensional deformation processes like fiber spinning and film blowing as well was discovered and named as such in 1960s and ever since rigorously investigated both theoretically and experimentally during the last four decades by many researchers throughout the world due to its direct connections to the industrially important productivity issues and to the academically intriguing stability topics, spearheaded notably by the three different prominent groups of Pearson, Agassant, and Co [Agassant *et al.* (2005); Anturkar and Co (1988); Barq *et al.* (1994); Co (2005); Iyengar and Co (1996); Jung and Hyun (2005, 2006); Pearson (1985)].

The neck-in and the edge bead on the film width are caused by the asymmetry in the extensional deformation between the center and the edge of the film width [Doborth and Erwin (1986)]. All of the above three phenomena lead to the detrimental effects on the uniformity of final film product, which should be eliminated or minimized for the sake of stable, efficient production process of film casting [Jung *et al.* (1999); Lee *et al.* (2004)].

While the draw resonance instability and the neck-in can be studied by one-dimensional (1D) simulation models (with varying width) of the system as first demonstrated by the comprehensive studies by Silagy *et al.* (1996, 1998) and recently by Lee *et al.* (2001), where the distance in the machine direction along with time constitutes the

two independent variables of the governing (partial differential) equations of the system, the edge bead can only be studied with two-dimensional (2D) [or three-dimensional (3D)] simulation models where either two spatial coordinate variables of x (machine direction) and y (traverse, i.e., film width direction) or three spatial coordinate variables of x, y, and z (film thickness direction), along with time constitute the three (or four) independent variables for the 2D (or 3D) model systems [Chae *et al.* (2000); Kim *et al.* (2005); Sakaki *et al.* (1996); Satoh *et al.* (2001); Silagy *et al.* (1998); Sollogoub *et al.* (2006)]. The studies on film casting to date can be classified according to these criteria, i.e., how many independent variables, whether constant width or varying width model, whether isothermal or nonisothermal conditions [Lamberti *et al.* (2001); Smith and Stolle (2000); Sollogoub *et al.* (2003)], whether viscoelastic model or not, etc.

The present study represents an extension of our earlier report [Kim *et al.* (2005)] where a 2D, upper-convected Maxwell (UCM) simulation model was solved to produce for the first time the transient as well as steady state solutions of the dynamics in film casting, making possible the investigation of the effects of various process and material parameters on the dynamic behavior of the system. The present study additionally addresses two important features in the simulation study on film casting, i.e., nonisothermal process conditions and the differentiation of extension-thickening and extension-thinning fluids in their different behavior in film casting. This is possible thanks to the Phan-Thien-Tanner (PTT) model portraying both types of fluids, whereas UCM does only extension-thickening ones [Phan-Thien (1978)].

II. MATHEMATICAL MODELING

The dimensionless governing equations of film casting process investigated in the present study are as follows: the continuity and motion equations and the boundary conditions are the same as those used by Kim *et al.* (2005) while the PTT replaces the UCM constitutive equation and the energy equation is newly added to the system. Figure 1 illustrates the schematic geometry and boundaries of the system.

Equation of continuity:

$$\frac{\partial e}{\partial t} + \nabla \cdot e\boldsymbol{v} = 0, \tag{1}$$

where

$$e = \frac{\bar{e}}{\bar{e}_0}, \quad \boldsymbol{v} = \frac{\bar{\boldsymbol{v}}}{\bar{v}_0}, \quad t = \frac{\bar{t}\bar{v}_0}{\bar{w}_0}, \quad \nabla = \frac{\bar{\nabla}}{\bar{w}_0}.$$

Equation of motion:

$$\nabla \cdot e\boldsymbol{\sigma} = 0, \tag{2}$$

where

$$\boldsymbol{\sigma} = \frac{\bar{\boldsymbol{\sigma}}\bar{w}_0}{\eta_0\bar{v}_0}$$

TABLE I. Process conditions and values of parameters.

Parameters	Values
Die gap[a] ($\bar{e}_0$), m	0.001
Half die width,[a] ($\bar{w}_0$), m	0.05
Extrusion velocity,[b] ($\bar{v}_0$), m/s	0.002
Extrusion temperature,[b] ($\bar{\theta}_0$), K	473.15
Ambient air temperature,[b] ($\bar{\theta}_a$), K	298.15
Material relaxation time (λ_0)[f] of LDPE at 473.15 K, s	0.075
Material relaxation time (λ_0)[f] of HDPE at 473.15 K, s	0.025
Activation energy (E_a)[c] of LDPE, KJ/mol	45
Activation energy (E_a)[c] of HDPE, KJ/mol	35
Heat capacity (C_p)[c] LDPE, KJ/(kg K)	1.90
Heat capacity (C_p)[c] of HDPE, KJ/(kg K)	1.56
Zero-shear viscosity (η_0)[c] of LDPE at 473.15 K, Pa·s	11 333
Zero-shear viscosity (η_0)[c] of HDPE at 473.15 K, Pa·s	8666
Heat transfer coefficient ($\bar{h}$)[d] of LDPE, W/(m^2 K)	14.35
Heat transfer coefficient ($\bar{h}$)[c] of HDPE, W/(m^2 K)	2.87
PTT model parameter,[e] ε	0.015
PTT model parameter,[g] ξ	0.1 (LDPE), 0.7 (HDPE)

[a]Equipment specifications by the manufacturer, Collin Co., Germany.
[b]Experimental operating conditions in this study.
[c]The material data provided by the polymer manufacturer LG Chem, Korea.
[d]Sollogoub, C., Y. Demay, and J. F. Agassant, "Non-isothermal viscoelastic numerical model of the cast-film process," J. Non-Newtonian Fluid Mech. **138**, 76–86 (2006).
[e]Phan-Thien, N., "A nonlinear network viscoelastic model," J. Rheol. **22**, 259–283 (1978).
[f]Relaxation time (λ_0) is determined by the reciprocal frequency at the intersection of storage modulus (G') and loss modulus (G'') curves.
[g]The value of ξ is determined best fitting the Rheotens curves of polymers as shown in Fig. 2.

Rheological constitutive equation:

PTT model:

$$K\boldsymbol{\tau} + De\left[\frac{\partial \boldsymbol{\tau}}{\partial t} + \boldsymbol{v}\cdot\nabla\boldsymbol{\tau} - \boldsymbol{L}\cdot\boldsymbol{\tau} - \boldsymbol{\tau}\cdot\boldsymbol{L}^T\right] = 2\frac{De}{De_0}\boldsymbol{D}, \tag{3}$$

where

$$\boldsymbol{\tau} = \frac{\bar{\boldsymbol{\tau}}\bar{w}_0}{\eta_0\bar{v}_0}, \quad K = \exp[\varepsilon De_0 \mathrm{tr}\,\boldsymbol{\tau}], \quad \boldsymbol{L} = \nabla\boldsymbol{v} - \xi\boldsymbol{D}, \quad 2\boldsymbol{D} = [(\nabla\boldsymbol{v}) + (\nabla\boldsymbol{v})^T],$$

$$\eta = \eta_0 \exp\left[\frac{E_a}{R\bar{\theta}_0}\left(\frac{1}{\theta} - 1\right)\right], \quad \lambda = \frac{\eta}{G} = \lambda_0 \exp\left[\frac{E_a}{R\bar{\theta}_0}\left(\frac{1}{\theta} - 1\right)\right],$$

$$De_0 = \frac{\lambda_0\bar{v}_0}{\bar{w}_0}, \quad De = \frac{\lambda\bar{v}_0}{\bar{w}_0} = De_0 \exp\left[\frac{E_a}{R\bar{\theta}_0}\left(\frac{1}{\theta} - 1\right)\right].$$

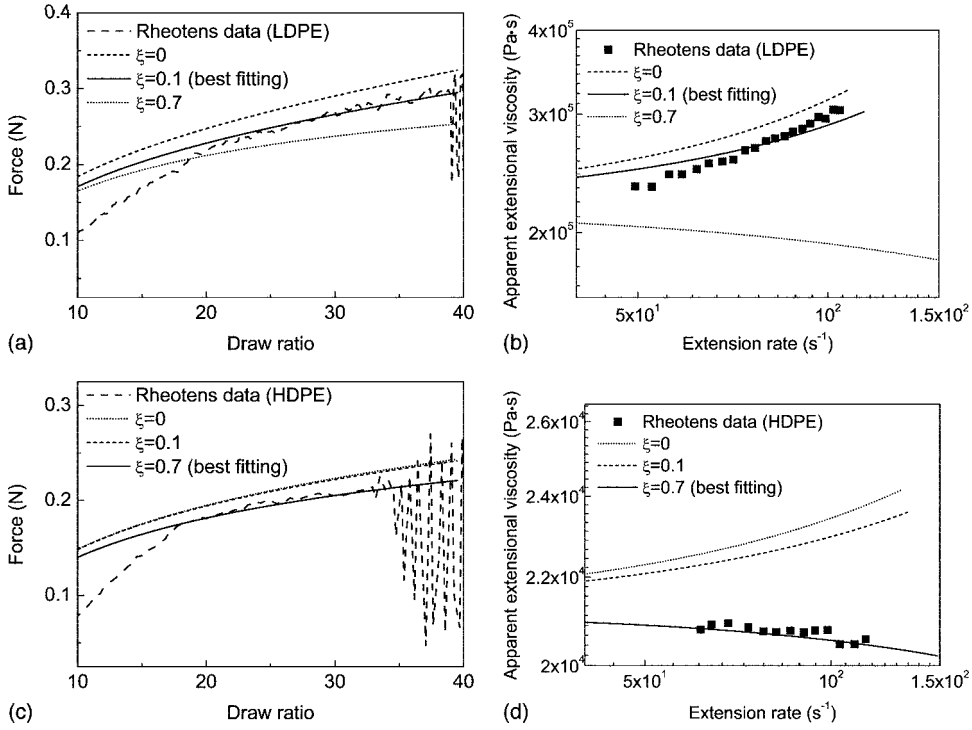

FIG. 2. Determination of the PTT model parameter ξ best fitting the tensile force and extensional viscosity data from Rheotens (a) curve fitting of LDPE (extension-thickening) curves, (b) apparent extensional viscosity curves of LDPE obtained from (a), (c) curve fitting of HDPE (extension-thinning) curves, and (d) apparent extensional viscosity curves of HDPE obtained from (c).

Equation of energy:

$$\frac{\partial \theta}{\partial t} + \boldsymbol{v} \cdot \nabla \theta = -\frac{h}{e}(\theta - \theta_a), \tag{4}$$

where

$$\theta = \frac{\bar{\theta}}{\bar{\theta}_0}, \quad \theta_a = \frac{\bar{\theta}_a}{\bar{\theta}_0}, \quad h = \frac{2\bar{h}\bar{w}_0}{\rho C_p \bar{v}_0 \bar{e}_0}.$$

Boundary conditions:

(i) Inlet:

$$v_x = 1, \quad v_y = 0, \quad e = 1, \quad w = 1, \quad \theta = 1, \quad \boldsymbol{\tau} = \boldsymbol{\tau}_0 \quad \text{on } \partial\Omega_1 \text{ at } t = 0. \tag{5a}$$

$$v_x = 1, \quad v_y = 0, \quad e = 1, \quad w = 1, \quad \theta = 1 \quad \text{on } \partial\Omega_1 \text{ at } t > 0, \tag{5b}$$

where

$$w = \frac{\bar{w}}{\bar{w}_0}.$$

(ii) Outlet:

$$v_x = D_r, \quad v_y = 0 \quad \text{on } \partial\Omega_2 \text{ at } t = 0. \tag{5c}$$

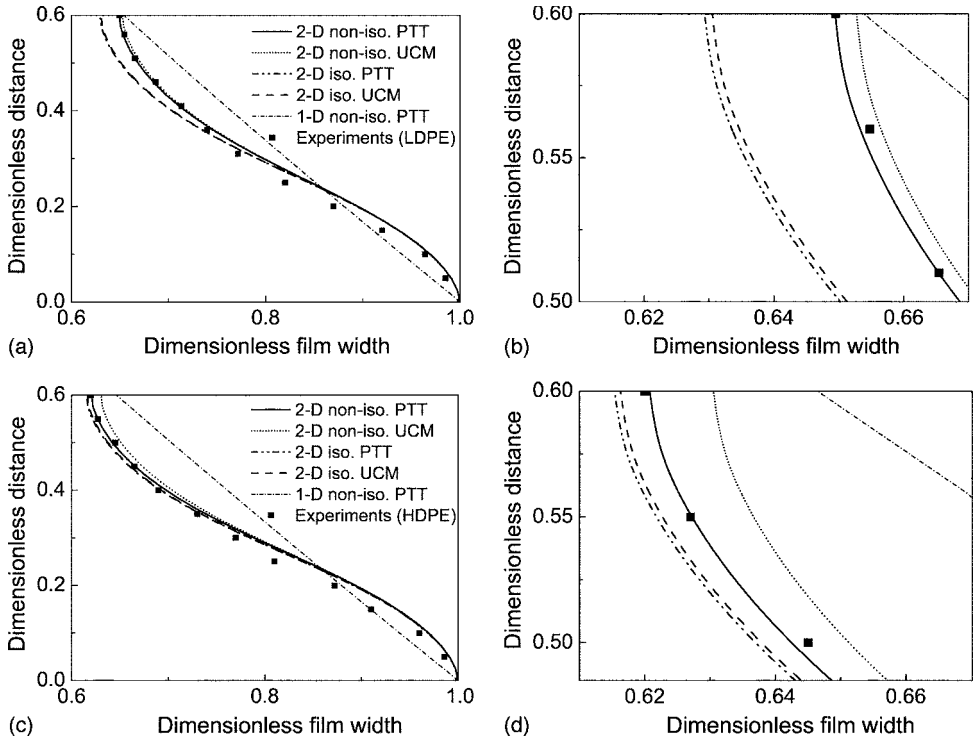

FIG. 3. Comparison between simulation (isothermal and nonisothermal models) and experimental results: film width profiles for (a) LDPE film casting, (b) magnified picture of (a), (c) HDPE film casting, and (d) magnified picture of (c) [$\bar{v}_0$=0.002 m/s, $\bar{e}_0$=0.001 m, $\bar{w}_0$=0.05 m, $\bar{\theta}_0$=473.15 K, A_r=0.6, D_r=10, De_0=0.003 (LDPE) and 0.001 (HDPE), h=0.5 (LDPE) and 0.1 (HDPE), ε=0.015, ξ=0.1 (LDPE) and 0.7 (HDPE)].

$$v_x = D_r(1+\delta), \quad v_y = 0 \quad \text{on } \partial\Omega_2 \text{ at } t > 0, \tag{5d}$$

where

$$D_r = \frac{\bar{v}_L}{\bar{v}_0}.$$

(iii) Center:

$$\sigma_{xy} = 0 \quad \text{on } \partial\Omega_3 \text{ at } t \geqslant 0. \tag{5e}$$

(iv) Edge:

$$\frac{\partial w}{\partial t} + v_x \frac{\partial w}{\partial x} = v_y, \quad \boldsymbol{\sigma}\cdot\boldsymbol{n} = 0 \quad \text{on } \partial\Omega_4 \text{ at } t \geqslant 0, \tag{5f}$$

where e denotes the dimensionless film thickness, w dimensionless film width, t dimensionless time, $\boldsymbol{v}$ dimensionless velocity vector with components v_x and v_y in x and y directions, $\boldsymbol{\sigma}$ dimensionless total stress tensor, $\boldsymbol{\tau}$ dimensionless extra stress tensor, $\boldsymbol{D}$ dimensionless strain rate tensor, ε and ξ the PTT model parameters, De Deborah number, η_0 zero-shear viscosity, λ fluid relaxation time, G modulus, E_a activation energy, R gas constant, θ dimensionless temperature, θ_a dimensionless ambient air temperature, h dimensionless heat transfer coefficient, ρ fluid density, C_p heat capacity, D_r draw ratio ($\equiv\bar{v}_L/\bar{v}_0$), δ a step change in take-up velocity initiating transient response of the system,

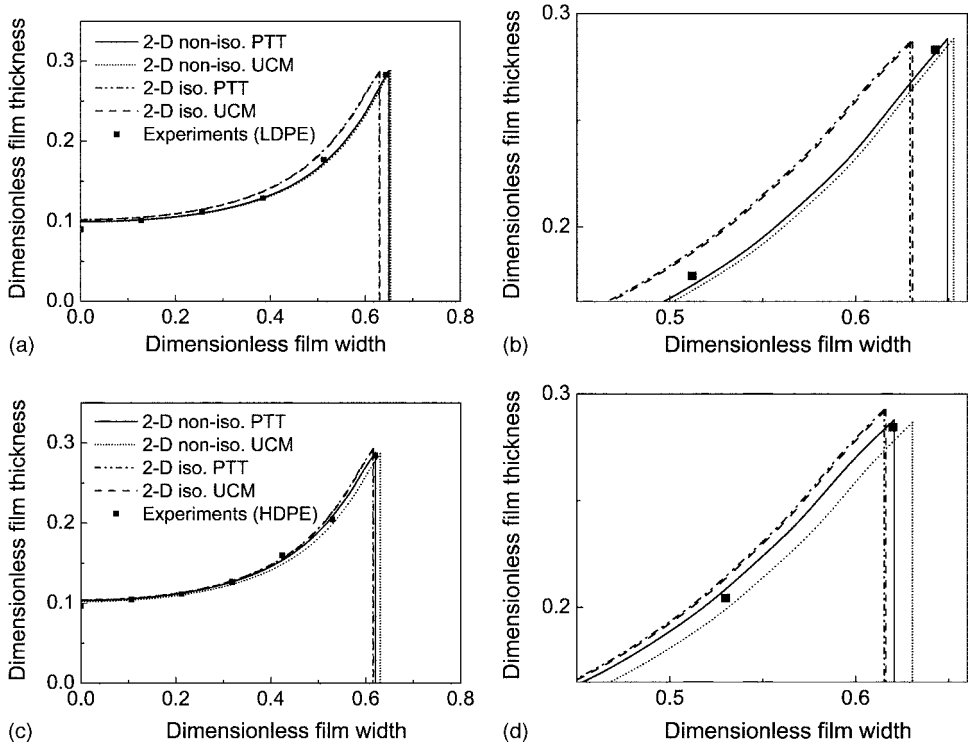

FIG. 4. Comparison between simulation (isothermal and nonisothermal models) and experimental results: edge bead profiles for (a) LDPE film casting, (b) magnified picture of (a), (c) HDPE film casting, and (d) magnified picture of (c) with the same conditions of Fig. 3.

and $\boldsymbol{n}$ normal vector. Overbars denote dimensional variables. Subscripts 0 and L denote die exit and chill roll position, respectively. Subscripts x, y and z represent the flow (machine direction), transverse (film width direction), and normal directions (film thickness direction), respectively. It is noted that the modulus has been assumed a constant value based on the fact that its temperature dependency is much smaller than that of the viscosity [Muslet and Kamal (2004)]. And the viscosity and the relaxation time are then the functions of temperature.

In this 2D model, it is assumed that the state variables do not vary in the film thickness direction, and the total stress in this thickness direction (σ_{zz}) should be zero, meaning that the isotropic pressure (P) is equal to the deviatoric normal stress (τ_{zz}). The secondary forces on the film such as gravity, surface tension, air drag, inertia, etc., are neglected in this study. The gravity force can substantially affect the film casting dynamics if the aspect ratio ($A_r \equiv L/\bar{w}_0$) is increased [Barq *et al.* (1994)]. However, it is negligible in the force balance in this study conducted on small desk top film casting equipment. The heat transfer between the film and the ambient air has been treated as the constant average value along the spatial coordinates since the cooling effects are considered to enter the system dynamics in an average sense.

III. NUMERICAL METHODS

All the numerical finite element methods (FEMs) and schemes employed in the present study for studying 2D, nonisothermal, and PTT simulation model are the same as

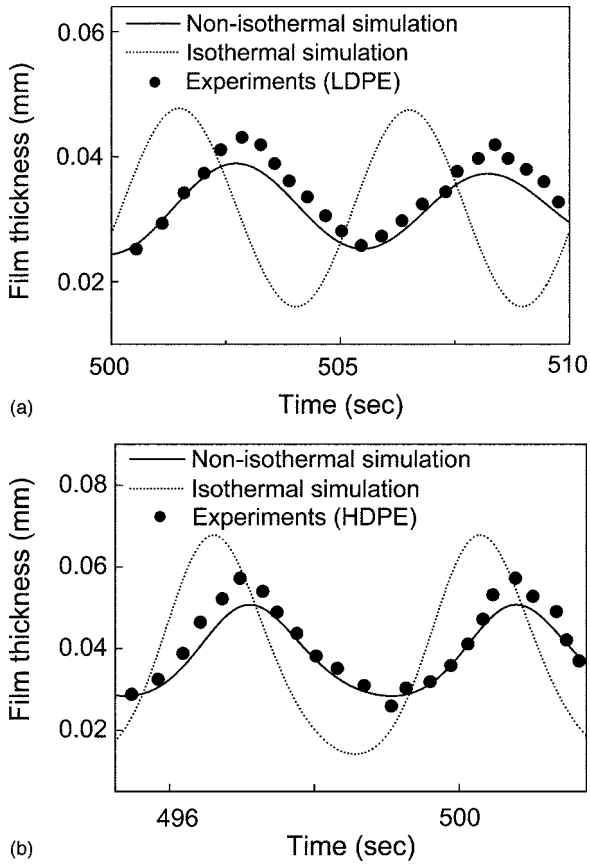

FIG. 5. Temporal center thickness profiles of (a) LDPE, and (b) HDPE film casting in draw resonance instability, showing the close agreement between experiments and simulation, i.e., for LDPE period by simulation, T=4.31 s, period by experiments, T=4.15 s; for HDPE period by simulation, T=3.69 s, period by experiments, T=3.75 s (D_r=30, and the other conditions are the same as in Fig. 3).

in Kim *et al.* (2005) where for the first time transient solutions were reported for an isothermal and UCM model system: spine and arbitrary Lagrangian Eulerian algorithm for free surface tracking, streamline upwinding/Petrov Galerkin method for numerically stabilizing convective terms in the continuity and kinematic conditions, an unconditionally stable second-order Gear method for time discretization. The stress boundary conditions at die exit are treated as unknowns to be determined through iterations starting from the initial guess of Newtonian values and ending when the draw ratio is satisfied at the take-up. These numerical methods are referred to Kim *et al.* (2005) for details.

IV. RESULTS AND DISCUSSION

The values of the parameters involved in the simulation model are described in Table I. Of the two PTT model parameters (ε and ξ), the value of ξ has been determined as best fitting the tensile force and apparent extensional viscosity data from the Rheotens [Doufas (2006)] instead of the extensional viscosity curves from extensional rheometers, i.e., rheometrics melt extensional rheometer (RME). This is because the Rheotens data can easily cover the high extension rate ranges exhibited in film casting process whereas the extensional rheometers can realize the relatively low extension rates only. Figure 2 shows

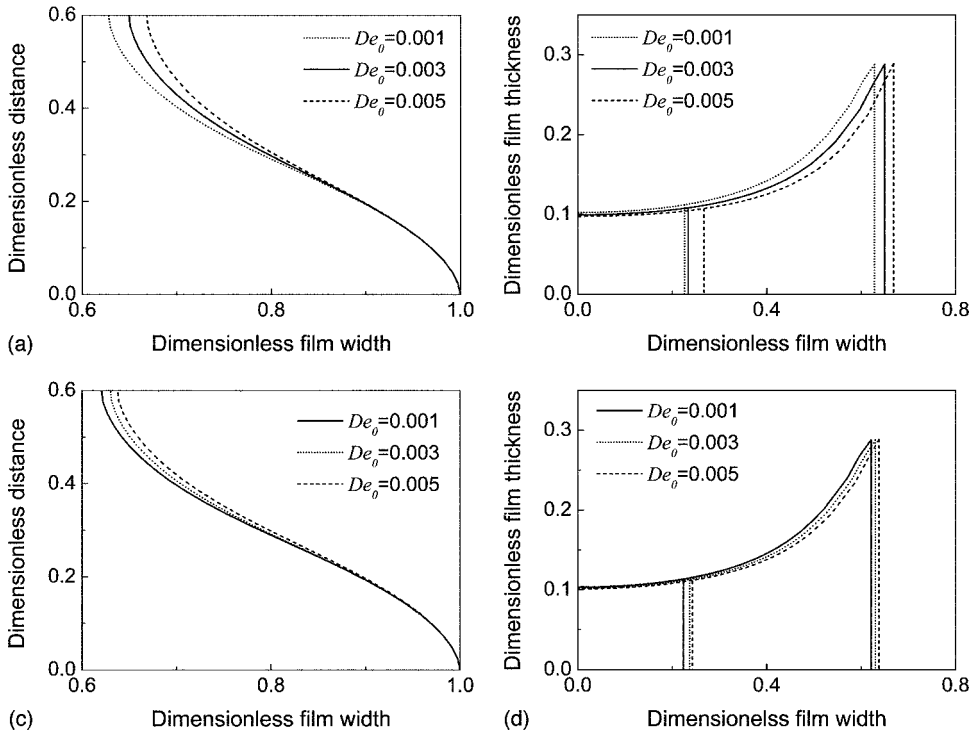

FIG. 6. Steady state profiles showing neck-in and edge bead for extension-thickening and -thinning fluids with different fluid viscoelasticity, De_0: (a) neck-in of extension-thickening fluids, (b) edge bead of extension-thickening fluids, (c) neck-in of extension-thinning fluids, and (d) edge bead of extension-thinning fluids [$\bar{\theta}_0$ =473.15 K, A_r=0.6, D_r=10, h=0.5 (LDPE) and 0.1 (HDPE), ε=0.015, ξ=0.1 (LDPE) and 0.7 (HDPE)].

how the value of ξ has been determined for LDPE and HDPE using the Rheotens data, i.e., ξ=0.1 for LDPE and 0.7 for HDPE polymers. The value of ε has been set to 0.015 following the suggestion by the author of the PTT model [Phan-Thien (1978)].

Figure 3 shows the comparison between experimental results of the film width profiles with those by various simulation models, i.e., 1D nonisothermal PTT, 2D isothermal UCM and PTT, 2D nonisothermal UCM and PTT models. The simulation results by the last model in the above, i.e., the present study, most favorably fit the experimental data of both LDPE and HDPE films since it incorporates the extension-thickening and extension-thinning features of the PTT model along with the nonisothermal cooling conditions.

Figure 4 displays another comparison of experimental results with those by simulation models, the edge bead, i.e., the nonuniform film thickness in the width direction. Again the simulation model of this study exhibits the best fit of the experimental data of both LDPE and HDPE films, as they should. While Figs. 3 and 4 demonstrate the utility of the simulation model of this study in fitting the steady state experimental data of film casting, Fig. 5 shows the utility in fitting the dynamic experimental data, especially during the draw resonance instability oscillations. This kind of comparison is possible only when the transient solutions of the dynamics in film casting process are available. Together with the previous paper by Kim *et al.* (2005), the present study presents the transient dynamic solutions of the film casting solving 2D partial differential equations by employing a FEM equipped with other numerical schemes as explained in Kim *et al.* (2005).

The two basic characteristics of the transient solutions during the draw resonance

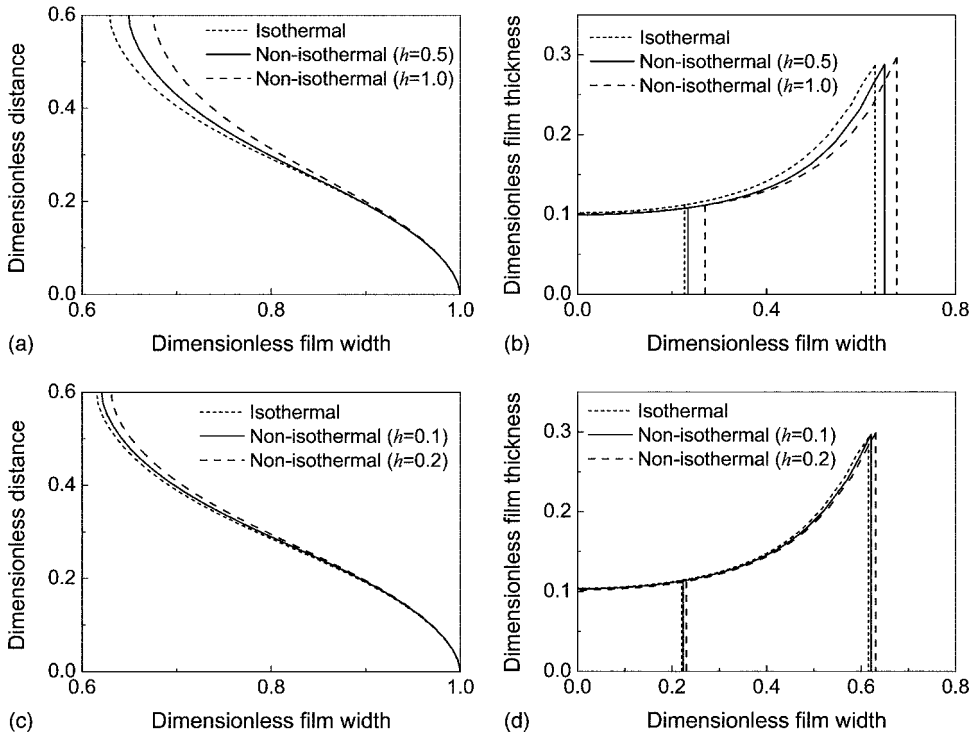

FIG. 7. Steady state profiles for nonisothermal conditions in comparison with isothermal conditions (a) neck-in of extension-thickening fluids, (b) edge bead of extension-thickening fluids, (c) neck-in of extension-thinning fluids, and (d) edge bead of extension-thinning fluids [$\bar{\theta}_0$=473.15 K, A_r=0.6, D_r=10, De_0=0.003 (LDPE) and 0.001 (HDPE), ε=0.015, ξ=0.1 (LDPE) and 0.7 (HDPE)].

oscillations, the severity and the period of the oscillations, have been compared with the experimental data for both LDPE and HDPE film casting. Again, the agreement is quite good considering the fact that there are assumptions and approximations incorporated in the simulation model, confirming that the PTT constitutive model turns out to be quite adequate for portraying the behavior, both steady state and dynamic (transient), of film casting.

Now that it has been found that the film casting process is well described by the simulation model in the present study, both steady state and dynamic, the next thing is to conduct a sensitivity study of the process using the model. That is, the effects of the various process and material parameters on the steady state or transient behavior of film casting have been investigated: the viscoelasticity of the polymer, the cooling conditions, and the aspect ratio defined as the distance between the die exit and the chill roll divided by the film width. Figures 6–8 illustrate the results of the above parameters on the steady state behavior in the film casting process, while Figs. 9–11 illustrate the results on the transient behavior. Figure 6 shows the effect of the Deborah number on neck-in and edge bead in both extension-thickening and -thinning fluids. The effect of cooling on the same neck-in and edge bead is shown in Fig. 7, while the effect of the aspect ratio is shown in Fig. 8. In Figs. 6–8 the trimming points are indicated where excessive edge beads are trimmed away for uniform film thickness. It has been found that as Deborah number and cooling increase or the aspect ratio decreases, the degree of neck-in in film width decreases, thus reducing the trimmed-away portions of the film product.

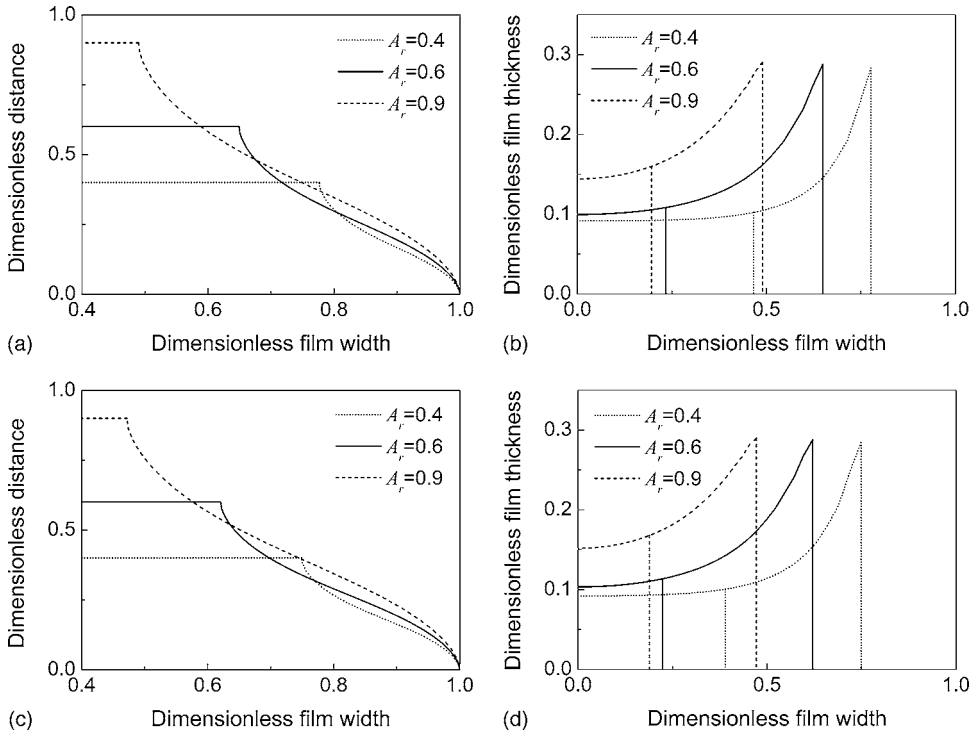

FIG. 8. Steady state profiles showing neck-in and edge bead for extension-thickening and -thinning fluids with different aspect ratios, A_r: (a) neck-in of extension-thickening fluids, (b) edge bead of extension-thickening fluids, (c) neck-in of extension-thinning fluids, and (d) edge bead of extension-thinning fluids [$\bar{\theta}_0$=473.15 K, D_r=10, De_0=0.003 (LDPE) and 0.001 (HDPE), h=0.5 (LDPE) and 0.1 (HDPE), ε=0.015, ξ=0.1 (LDPE) and 0.7 (HDPE)].

The effect of the Deborah number on the transient behavior of the system is illustrated in Fig. 9 in that the *De* stabilizes the system for the extension-thickening fluids, whereas it destabilizes for the extension-thinning fluids [Lee *et al.* (2001)]. The cooling always exerts a stabilizing effect in both extension-thickening as shown in Fig. 10 and -thinning fluids [Jung *et al.* (1999); Lee *et al.* (2000)]. The aspect ratio also exerts a stabilizing effect in both extension-thickening, as shown in Fig. 11, and extension-thinning fluids.

Finally, it is worth mentioning here, after the results reported in this paper, what the next step will be in developing the most suitable simulation model for film casting. The logical step is to incorporate the flow-induced crystallization (FIC) into the model, because this FIC has been successfully studied recently in other extensional deformation processes like fiber spinning to yield satisfactory results. The simulation results, both steady state and transient, by FIC-included model for fiber spinning describe fairly well the spinline profiles of state variables like stress, temperature, diameter and crystallinity [Lee *et al.* (2005); Shin *et al.* (2005)]. Also, the famous nonlinear phenomenon called the neck-like deformation occurring on the high speed spinline was satisfactorily produced by the FIC-included simulation model without having to assume any artificially high viscosity values on the spinline [Kohler *et al.* (2005); Shin *et al.* (2006)].

V. CONCLUSIONS

The simulation model equipped with the PTT constitutive equation capable of differentiating between extension-thickening (strain-hardening) and extension-thinning (strain-

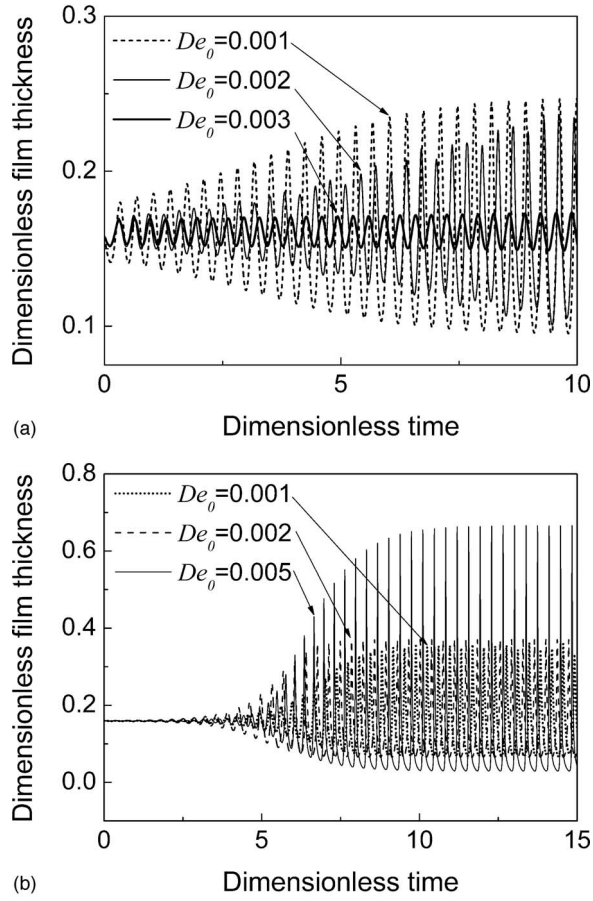

FIG. 9. Effect of fluid viscoelasticity, De_0 on the stability for (a) extension-thickening fluids, and (b) extension-thinning fluids [$\bar{\theta}_0$=473.15 K, A_r=0.6, D_r=30, h=0.5 (LDPE) and 0.1 (HDPE), ε=0.015, ξ=0.1 (LDPE) and 0.7 (HDPE)].

softening) fluids has been established to describe 2D viscoelastic nonisothermal film casting process. Thus produced simulation results are quite satisfactory in agreeing fairly well with experimental data of LDPE and HDPE film casting, both steady state and transient solutions. Especially, thanks to the transient solutions of the dynamics in nonisothermal film casting by this study, the first reported in the literature, the various aspects of the dynamic behavior in film casting can be investigated and analyzed including neck-in and edge bead on the film width, and draw resonance oscillation. The sensitivity analysis on the effects of process and material parameters on the dynamics of the system is also readily possible with the simulation model. The next logical step in enhancing the simulation model is to include the flow-induced crystallization (FIC) which recently has been proven successfully, being incorporated into other extensional deformation processes. The results of FIC-included model will be reported in the sequel of this paper.

ACKNOWLEDGMENTS

This study was supported by research grants from the Korea Science and Engineering Foundation (KOSEF) through the Applied Rheology Center (ARC), an official KOSEF-created engineering research center (ERC) at Korea University, Seoul, Korea.

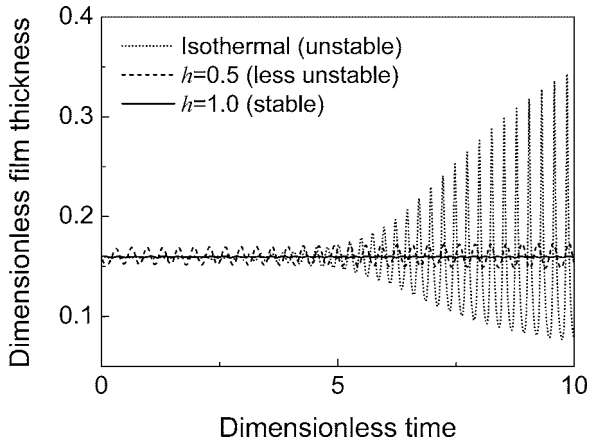

FIG. 10. Effect of cooling of the film on the stability ($\bar{\theta}_0$=473.15 K, A_r=0.6 D_r=30, De_0=0.003, ε=0.015, ξ=0.1).

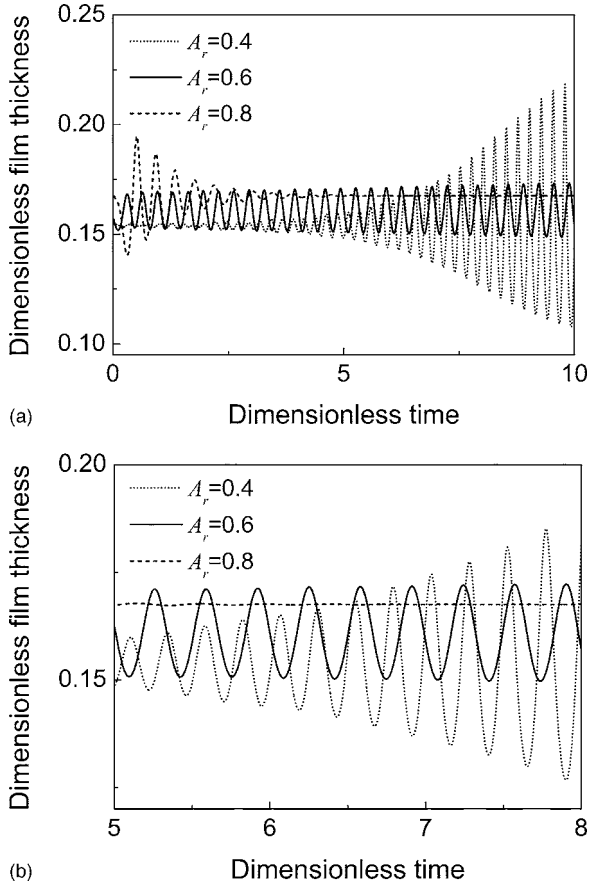

FIG. 11. (a) Effect of aspect ratio, A_r on the stability ($\bar{\theta}_0$=473.15 K, D_r=30, De_0=0.003, h=0.5, ε=0.015, ξ=0.1), and (b) magnified picture of (a).

References

Agassant, J. F., Y. Demay, C. Sollogoub, and D. Silagy, "Cast film extrusion—An overview of experimental and theoretical approaches," Int. Polym. Process. **20**, 136–148 (2005).

Anturkar, N. R., and A. Co, "Draw resonance in film casting of viscoelastic fluids: A linear stability analysis," J. Non-Newtonian Fluid Mech. **28**, 287–307 (1988).

Barq, P., J. M. Haudin, J. F. Agassant, and P. Bourgin, "Stationary and dynamic analysis of film casting process," Int. Polym. Process. **9**, 350–358 (1994).

Chae, K. S., M. H. Lee, S. J. Lee, and S. J. Lee, "Three-dimensional numerical simulation for the prediction of product shape in sheet casting process," Korea-Aust. Rheol. J. **12**, 107–117 (2000).

Co, A., "Draw resonance in film casting," in *Polymer Processing Instabilities*, edited by S. G. Hatzikiriakos and K. B. Migler (Dekker, New York, 2005).

Dobroth, T., and L. Erwin, "Causes of edge beads in cast films," Polym. Eng. Sci. **26**, 462–467 (1986).

Doufas, A. K., "Analysis of the rheotens experiment with viscoelastic constitutive equations for probing extensional rheology of polymer melts," J. Rheol. **50**, 749–769 (2006).

Iyengar, V. R., and A. Co, "Film casting of a modified Giesekus fluid: Stability analysis," Chem. Eng. Sci. **51**, 1417–1430 (1996).

Jung, H. W., H.-S. Song, and J. C. Hyun, "Analysis of stability effect of spinline cooling in melt spinning," J. Non-Newtonian Fluid Mech. **87**, 165–174 (1999).

Jung, H. W., and J. C. Hyun, "Fiber spinning and film blowing instabilities," in *Polymer Processing Instabilities*, edited by S. G. Hatzikiriakos and K. B. Migler (Dekker, New York, 2005).

Jung, H. W., and J. C. Hyun, "Instabilities in extensional deformation polymer processing," in *Rheology Reviews*, edited by D. M. Binding and K. Walters (The British Society of Rheology, Aberystwyth, 2006).

Kim, J. M., J. S. Lee, D. M. Shin, H. W. Jung, and J. C. Hyun, "Transient solutions of the dynamics of film casting process using a 2–D viscoelastic model," J. Non-Newtonian Fluid Mech. **132**, 53–60 (2005).

Kohler, W. H., P. Shrikhande, and A. J. McHugh, "Modeling melt spinning of PLA fibers," J. Macromol. Sci., Phys. **44**, 185–202 (2005).

Lamberti, G., G. Titomanlio, and V. Brucato, "Measurement and modeling of the film casting process 1. Width distribution along draw direction," Chem. Eng. Sci. **56**, 5749–5761 (2001).

Lee, J. S., H. W. Jung, and J. C. Hyun, "Melt spinning dynamics of Phan-Thien-Tanner fluids," Korea-Aust. Rheol. J. **12**, 119–124 (2000).

Lee, J. S., H. W. Jung, H.-S. Song, K.-Y. Lee, and J. C. Hyun, "Kinematic waves and draw resonance in film casting process," J. Non-Newtonian Fluid Mech. **101**, 43–54 (2001).

Lee, J. S., H. W. Jung, and J. C. Hyun, "Stabilization of film casting by an encapsulation extrusion method," J. Non-Newtonian Fluid Mech. **117**, 109–115 (2004).

Lee, J. S., D. M. Shin, H. W. Jung, and J. C. Hyun, "Transient solutions of the dynamics in low-speed fiber spinning process accompanied by flow-induced crystallization," J. Non-Newtonian Fluid Mech. **130**, 110–116 (2005).

Muslet, I. A., and M. R. Kamal, "Computer simulation of the film blowing process incorporating crystallization and viscoelasticity," J. Rheol. **48**, 525–550 (2004).

Pearson, J. R. A., *Mechanics of Polymer Processing* (Elsevier, New York, 1985).

Phan-Thien, N., "A nonlinear network viscoelastic model," J. Rheol. **22**, 259–283 (1978).

Sakaki, K., R. Katsumoto, T. Kajiwara, and K. Funatsu, "Three-dimensional flow simulation of a film-casting process," Polym. Eng. Sci. **36**, 1821–1831 (1996).

Satoh, N., H. Tomiyama, and T. Kajiwara, "Viscoelastic simulation of film casting process for a polymer melt," Polym. Eng. Sci. **41**, 1564–1579 (2001).

Shin, D. M., J. S. Lee, H. W. Jung, and J. C. Hyun, "Analysis of the effect of flow-induced crystallization on the stability of low-speed spinning using the linear stability method," Korea-Aust. Rheol. J. **17**, 63–69 (2005).

Shin, D. M., J. S. Lee, H. W. Jung, and J. C. Hyun, "High-speed fiber spinning process with spinline flow-induced crystallization and neck-like deformation," Rheol. Acta **45**, 575–582 (2006).

Silagy, D., Y. Demay, and J. F. Agassant, "Study of the stability of the film casting process," Polym. Eng. Sci.

36, 2614–2625 (1996).

Silagy, D., Y. Demay, and J. F. Agassant, "Stationary and stability analysis of the film casting process," J. Non-Newtonian Fluid Mech. **79**, 563–583 (1998).

Smith, S., and D. Stolle, "Nonisothermal two-dimensional film casting of a viscous polymer," Polym. Eng. Sci. **40**, 1870–1877 (2000).

Sollogoub, C., Y. Demay, and J. F. Agassant, "Cast film problem: A non isothermal investigation," Int. Polym. Process. **18**, 80–86 (2003).

Sollogoub, C., Y. Demay, and J. F. Agassant, "Non-isothermal viscoelastic numerical model of the cast-film process," J. Non-Newtonian Fluid Mech. **138**, 76–86 (2006).